Contemporary Engineering Sciences, Vol. 13, 2020, no. 1, 39 - 58
HIKARI Ltd, www.m-hikari.com
https://doi.org/10.12988/ces.2020.91245

The Search for 'Defects' by Non-invasive Techniques: Development and Application of Pulsed-Transmissive and Reflective Thermography in Fiberglass Material

Gastón Sanglier Contreras*, Eduardo J. López Fernández
Sonia Cesteros García and Roberto A. González Lezcano

Departamento de Arquitectura y Diseño
Escuela Politécnica Superior
Universidad CEU San Pablo, Spain
* Corresponding author

Abstract

The application of thermography to the study of composite materials is a fact that is increasingly applied in different Non-Destructive Testing Laboratories (NDT). The application of heat pulses controlled by methods of transmission and reflection on the material and the study of the evolution of these pulses of heat over time, as well as the correct use of the thermography equipment as well as the conditions of contour, can show details that at first sight we are not able to perceive, for it is necessary to have a good test methodology. In this case thermographic tests have been carried out on a glass fiber radome (aeronautical material) in order to determine possible defects or indications such as cracks, delaminations, air pockets, etc. Following the principle of good practices to reduce as much as possible the number of tests to be applied to the inspection of an object, it is necessary to carry out a previous visual inspection for the possible detection of delaminations and detachments in an unpainted piece. The inspection by pulse-thermography shows a good behavior for the detection of breaks in the core in a piece painted by one or two faces.

Keywords: Pulse-thermography, composite materials, radome, fiberglass, non-invasive techniques

1 Introduction

Thermography is a non-destructive testing method (NDT) that allows to detect and measure temperature variations emitted by a body, transforming them into visible images. Obtaining these images (thermographs or thermograms) where controlled pulses of heat have been added by transmission and reflection methods to the part, as well as the necessary adjustments of the equipment, have allowed the collection of thermograms with the identification of possible 'defects' in a type of composite material such as a fibre-reinforced polymer.

There are several techniques to detect indications or 'defects' in different materials using infrared thermography. The difference between the different methods is mainly based on how the heat energy is transferred to the component to be tested in question. These methods can be classified as passive, active or vibrothermography [4,2,10,12].

The choice of a particular method depends on several factors, including the thermal characteristics of the body being inspected; the type, size and orientation of the defect to be located; the way in which the heat is induced in the body; the sensitivity and spatial resolution of the infrared images; and budgetary constraints.

Passive infrared thermography (PIR) is where no external heating or cooling stimulation is used to cause a flow of heat in the inspected body. The object under study produces a typical temperature pattern because it is involved in a (industrial) process that produces heat. A few degrees difference from the normal working (reference) temperature of the object shows unusual behaviour. Thermography is able to capture this temperature information in real time from a safe distance without any interaction with the object.

Passive IRR is used, for example, for product monitoring in manufacturing processes, monitoring welding processes or checking the efficiency of car brake discs. It can also be used in predictive maintenance, such as on bearings, turbines and compressors, electrical installations, buried pipelines or gas leaks. There are many other non-industrial applications, such as medical applications in the detection of breast cancer or vascular disorders, fire detection, target detection (military) or location of heat and humidity losses in buildings.

Active thermography requires external stimulation of the part to be inspected to cause a flow of heat in the part. An internal defect can alter that flow, causing an abnormal temperature distribution. There are different active thermography techniques depending on how the external heating or cooling of the part to be inspected is carried out (lock-in thermography, long pulse thermography, pulsed phase thermography and pulse-thermography) [1,11].

Vibrothermography is a technique based on lock-in thermography. Instead of heating the sample to be inspected by means of modulated light lamps, it uses an externally induced mechanical vibration. It is used for quality maintenance in the aerospace and automotive industry by monitoring the integrity of surface or subsurface features, which conventional NDT thermography cannot detect.

Vibrothermography allows to obtain images by means of thermal waves that are generated by elastic sound or ultrasonic waves. The mechanism involved is local or hysteresis friction that converts a dynamic load defect into a heat source, which is identified by a thermography system.

In this work we have not tried to make an exhaustive study of the different NDT techniques applied by means of infrared thermography. We will explain the development and use of the technique of pulse-thermography for the detection of possible defects or indications in a somewhat complex shaped piece of glass fibre composite material (Rohacell type), such as the radome of an aircraft, a piece that protects an antenna from the effects of its physical environment without damaging its electrical properties.

In pulsed thermography (PT) or pulse-thermography, the surface of the sample is subjected to a short heat pulse using a high energy source, such as photographic flashes. The pulse duration can vary from a few milliseconds (2-15 ms) to several seconds depending on the thermophysical properties of the sample and the defect [3,5,8,16].

After the thermal front contacts the sample surface, it travels from the surface through the sample. As time goes by, the defective areas will appear with a higher or lower temperature compared to non-defective areas of the surface, depending on the type of defect.

2 Materials and methods

Pulse-thermography consists of applying short pulses of heat to the surface of the part to be inspected, which increases the temperature of the analysis area. This heat pulse propagates below the surface through the process of diffusion and loss phenomena by radiation and convection. The speed of heat penetration into the material depends on some properties: heat capacity, thermal conductivity, density, material structure, etc. The duration of the heat pulse depends on the thickness of the material and its thermal properties.

Visual inspection by an operator is the most commonly adopted way of detecting possible defects in the different materials to be inspected. NDT organizations around the world have issued expert certification and qualification standards. For example, the American Society for Non-Destructive Testing (ASNT) recommends a certification level of capability in three tests for infrared personnel (thermographic

inspector level I, II and III). However, different automated methods can help reduce subjectivity and, in some cases, completely eliminate human intervention in the detection process [6,7].

Image analysis and processing equipment uses different techniques for better visualisation of 'defects' or indications on test pieces. These techniques include thresholding, segmentation, edge detection operators in pre-processing processes, methods for depth inversion in both the time and frequency domains, and statistical models. In the tests carried out in this work, adjustment methods have been used to improve the contrast between the defect and the reference of the part to be tested.

The presence of possible defects in the inspected piece (fibreglass radome), reduces the diffusion ratio, so that when the surface of the piece is observed, areas with different temperatures with respect to the bottom appear. The behaviour of the analysis area is observed by means of the different heat pulses, analysing the thermal increase in that area. The thermographic analysis of the piece was carried out by reflection (heating and observing a zone from the same site) and by transmission (heating and observing from opposite sites).

Both forms of heating and observation can be complementary, and will depend mainly on the depths of the surface at which the defects are found, and on the size of the defects so that they can be better observed on one side or the other of the inspected surface.

In a way, thermography has some similarity with the impulse-echo ultrasound technique, in the sense that the delayed signal disturbance produced by the subsurface defect can be considered as a reflection of the thermal wave by the defect, in time depending on the speed of propagation of the thermal wave (1):

$$v_{ter} \approx \frac{z}{t} \approx \left(\frac{\alpha}{t}\right)^{\frac{t}{2}} \approx \frac{\alpha}{z} \quad (1)$$

where 'z' is the depth of the fault, 't' is the elapsed time and 'α' is the thermal diffusion. The inspection time increases with the square of the defect Depth [13].
An important difference between ultrasonic and thermographic techniques is that thermal propagation is based on a diffusion equation rather than a wave equation, so the thermal wavelength is of the order of the depth of the thermal propagation. A consequence of this is that a porosity much smaller than the depth of the defect will also be much smaller than the thermal wavelength, so it will not affect the signal. A second consequence is that the thermographic technique will be relatively insensitive to subsurface defects whose diameter is smaller compared to their depth.

The difficulty of this methodology lies in fine-tuning the method, since many factors intervene: thickness of the material, depth and size of the defect, heating times, distances, emissivities, characteristics of the material, etc. A fine-tuning was made by making patterns and carrying out in them in a handmade way, the different

defects that were wanted to look for. These defects will appear by analyzing the different thermal image sequences, and looking for the highest thermal contrast, which sometimes was a few tenths of a degree.

The following equipment was used to carry out the tests:

- ThermaCam PM-595 thermal camera with high-speed image recording acquisition software (ThermaCam Researcher 2001).
- Heat source triggering controller (lamps).
- Hot spots with power of 1000 W each.

Figure 1: The image on the left shows the part analysed, a fibreglass radome. In the image on the right, the High Speed Thermal Imaging Equipment.

The thermal camera used to obtain the thermograms operated in the 7.5 to 13 μm range of the electromagnetic spectrum, with three temperature measurement ranges, and a thermal sensitivity of 0.1ºC. The type of detector used was a microbolometer-cooled 320*240 pixel FPA (Focal Plane Array). The images were obtained in digital format with a dynamic range of 14 bits, and the camera had the capacity to record 50 images per second for later study.

The shooting controller automated the sequence of turning on and off the heat sources, and set the respective times associated with those states. Two 1000 W lamps connected to the controller were used.
Two heating methods were used to observe the indications or possible defects in the part:

Transmission: in this type of test technique, the piece to be tested was heated on a different side from the one observed with the camera. Here we must distinguish between two forms of testing, which were called external transmission (te) and internal transmission (ti). The external transmission was carried out by heating the side without paint and observing with the camera on the painted side. The inner transmission was done by heating the painted side and looking at the unpainted side. The part to be examined (radome) was positioned on a trolley so that it was easy to move and manipulate it to change to the various inspection positions as required [13,14,15,17].

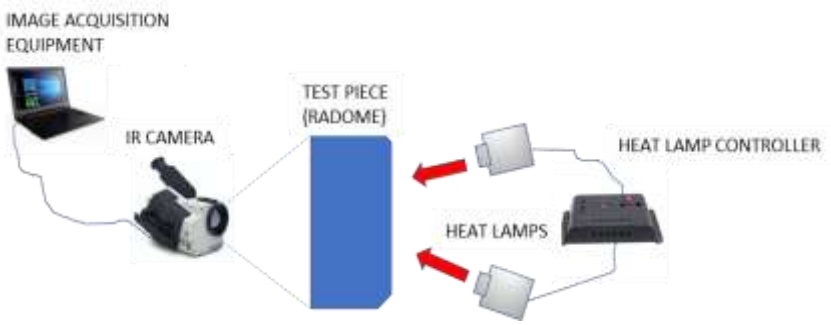

Figure 2: Equipment arrangement. Pulse-thermography by internal transmission.

Reflection: in this other type of test, the piece to be tested was heated on the same side as observed with the camera. Here again, two forms of test were distinguished, which were called external reflection (re) and internal reflection (ri). The external reflection was carried out by heating the side with paint and observing with the camera on the same side with paint. The interior reflection was done by heating the side not painted and observing with the camera on the same side. The piece to be tested was turned in the same way as the previous one

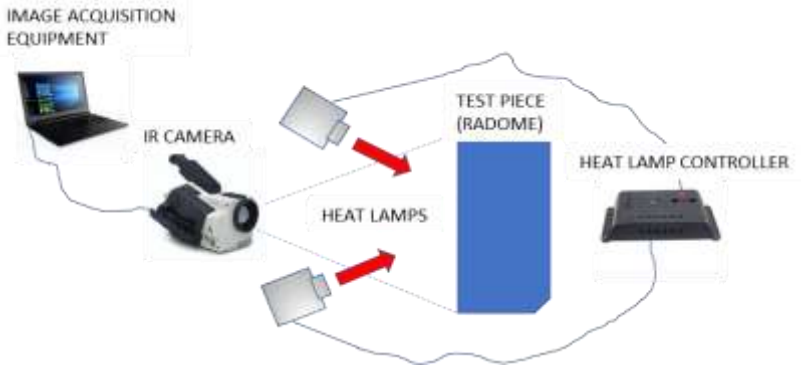

Figure 3: Equipment arrangement. Pulse-thermography by internal reflection.

Different sequences of images of the different areas of the part were recorded, and the first image (before heating) and the image where the contrast between the indications (defects) and the background (non-defective area) was greater was always chosen, repeatedly analysing the sequence to determine the moment of greatest thermal contrast. The choice of this comparative technique was made with the idea of eliminating the areas affected by the reflection, in addition to determining the possible defective areas. The test piece was painted on one side only, the convex side. This side was divided into different zones by means of aluminium tape. These areas were identified and subsequently analyzed. The aluminium tape was also used because of the good contrast to the background (painted white) due to the difference in emissivities between the two surfaces. The areas chosen were selected so that the possible indications sought in the piece (detachments, delaminations, overthickness, air and resin pockets) could be appreciated with an acceptable level of detail. For the inspection distance of 90 cm,

and using a 24º x 18º optic, a level of detail of 1.20 mm x 1.19 mm per pixel in the image was obtained [9].

3 Results

For the development of the test methodology, a specimen was manufactured from the same material as the part to be inspected, and with the same thicknesses for the development of the inspection method. Different defects were made in it: core breakage, detachments and holes at different depths. For the inspection of the specimen, it was divided into three zones, looking at the specimen from the front side, the upper left side was called A-zone, the central part B-zone, and finally the right side was called C-zone, as shown in the following figure 6.

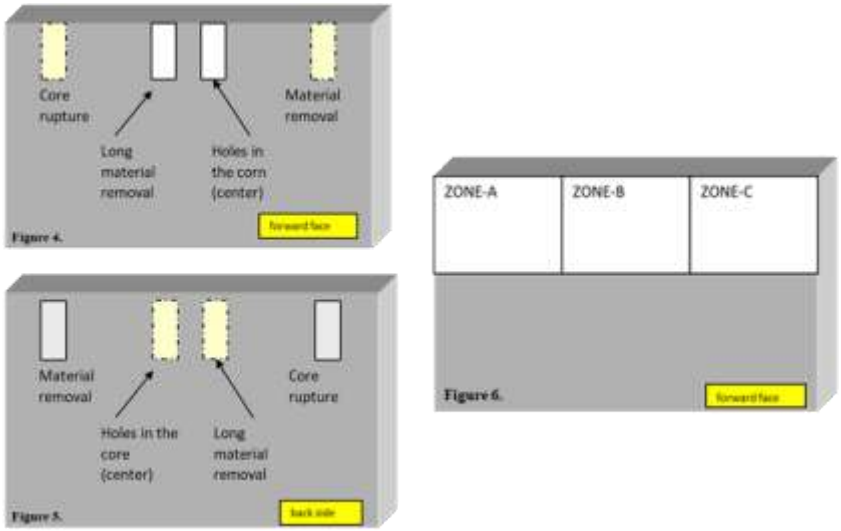

Figures 4, 5 and 6: Test tubes with different defects on the front side (figure 4) and on the back side (figure 5). Distribution of different zones with defects in the test piece (figure 6).

To obtain thermal images of the different areas, the camera was placed at a fixed distance from the front face of the specimen to be inspected. The heat lamp was positioned at a fixed distance of 15 cm from the front and back of the specimen (depending on the heating mode). The focus was fitted with lids so that the heat could be better concentrated in the area under analysis and the heating of the area could be as homogeneous as possible.

The determination of the exposure and rest times of the heat pulses was studied. Exposure time is understood as the time the light remains on, and therefore the time during which heat is contributed to the piece; and rest time is understood as the time the light remains off between pulses (no heat is contributed at that time).

The appropriate number of pulses was also studied, since it was necessary to determine when the area to be inspected was sufficiently heated without saturating the image obtained (thermogram).

It was verified that the maximum thermal contrasts between the different defects and the background were produced for an exposure time (te) of 4 seconds and a rest time (tr) of 0.5 seconds. The number of pulses was between one and nine, depending on the area of the piece to be inspected, in order to observe the evolution of the thermal gradient in the piece, and thus be able to detect the moment of greatest contrast in the image between the background of the piece and the possible defects or indications.

Thermal differences between the background and the defect were found to be around 0.2ºC and 0.5ºC, which made it very difficult to fine-tune the methodology, as the thermal contrasts were very small.

Next, the images obtained in the process of fine-tuning the method with the different tests carried out, and applying all the parameters that have been defined previously, will be presented.

Analysis of the reference test tube

At this point, the thermographies will be shown using the test tube for setting up the method by applying the different modes of heating by transmission and reflection explained above, and examining the test tube from both sides (figure 7 to figure 16).

The following thermal images have been obtained on the specimen to identify possible defects such as detachment, core breaks and delamination.

The analysis began by observing zone A of the test tube. Figure 7 shows the heating by external transmission, i.e. the part was heated from behind (unpainted side) and observed from the front (painted side).

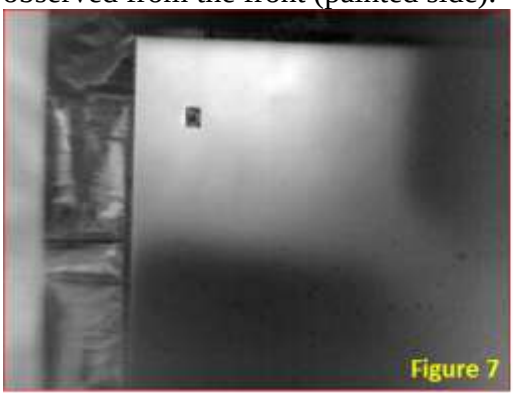

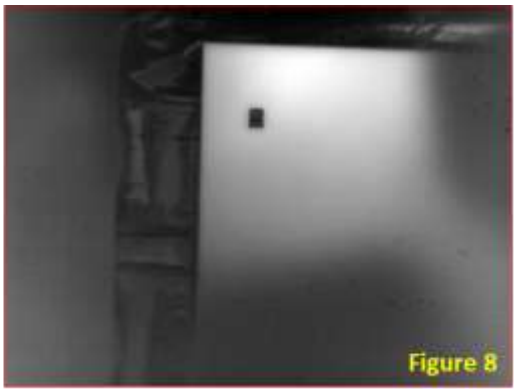

Figures 7 and 8: Image of the A-zone of the specimen taken by external transmisión (Figure 7) and the image of zone A of the test tube taken by external reflection (figure 8).

.

Figure 7 shows the defect, in this case a lift-off, with very little contrast, as it is located on the other side of the test tube, i.e. closer to the side where the area is

heated and not to the side where the surface is observed with the camera. A dark square appears corresponding to the aluminium tape which, due to its difference in emissivity with the paint on the surface to be inspected, helped to focus the camera and to serve as a scale (size H x W = 11mm x 8.5 mm) in the possible indications on the specimen.

Figure 8 shows the same area A, but with the difference that it has now been heated and viewed from the same side, i.e. front face or painted side. No indication (possible defects) has been observed there.

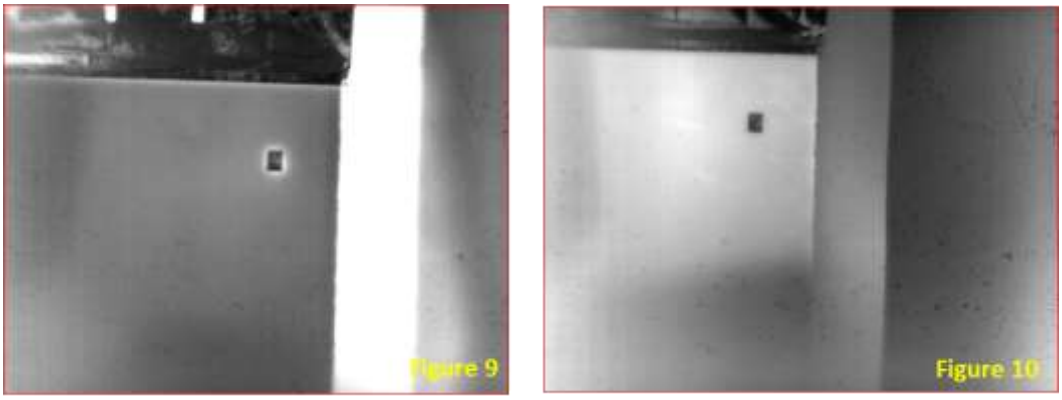

Figures 9 and 10: Image of the A-zone of the specimen taken by internal transmisión (figure 9) and the image of the A-zone of the test piece taken by internal reflection (figure 10).

Figure 9 shows a defect in the upper central part, but it is shown with very little contrast to that observed in figure 7. Subsequently, the test tube was turned over, heating the painted side and looking at the unpainted side. Figure 10 shows a higher contrast image of the defect, because it is closer to the face on the side facing the camera.

The four images shown below correspond to Zone B of the specimen. The heating effects, using active thermography and the order of analysis correspond to the same seen for the analysis of zone A.

In figure 11, if the upper part is seen to be lighter (heated), the take-off appears on the right of the image, while the holes are on the left. In this thermography it is verified that the takeoff is better detected, since a dark zone is observed, due to the accumulation of the material that has concentrated there after having made this defect of somewhat artisan form. In the defective part due to the holes, a marked zone is observed, but each hole cannot be distinguished individually (three holes were made at different depths). In the thermography of figure 12 no indication has been observed.

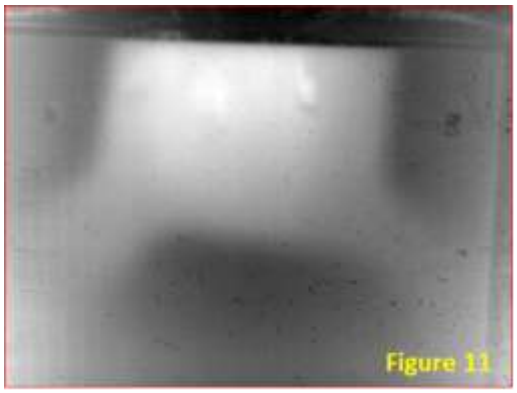

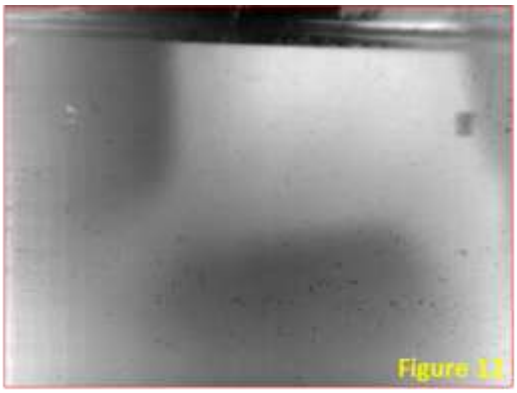

Figures 11 and 12: Image of the B-zone of the test piece taken by external transmisión (figure 11) and the image of the Zone-B of the test tube taken by external reflection (figura 12).

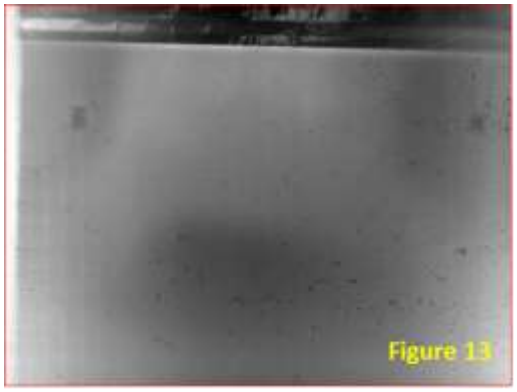

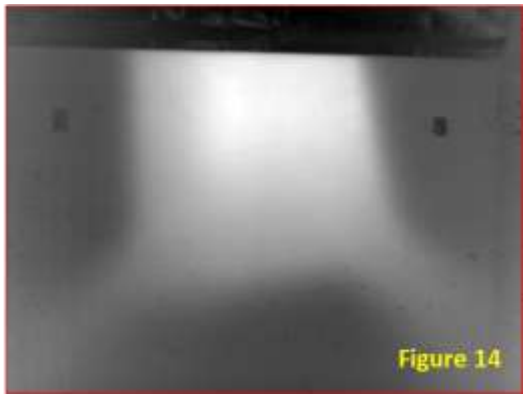

Figures 13 and 14: Image of the Zone-B of the test tube taken by internal transmisión (figure 13) and the image of the B-zone of the specimen taken by internal reflection (figure 14).
In the thermography of figure 13 the take-offs are observed, in addition to the zone of holes, but with less contrast than in figure 11. In the thermography of figure 14 there are no indications of possible defects, or defective areas.

Finally, the recorded thermographs of the zone C of the reference test tube are presented using the same methods as in the two previous zones.

In zone C, a core rupture of the material has been created as a defect. It can be seen, in figure 15, that the defect in the central part corresponding to the take-off is better seen than the defect in this zone, because it is closer to the surface observed by the camera.

In the two subsequent thermographies, which correspond to figures 16 and 17, there are no indications. However, in figure 18, next to the right of the black square of reference, a white rectangular zone can be seen (warmer due to the accumulation of heat in this zone) which corresponds to the defect generated there of core breakage of the material.

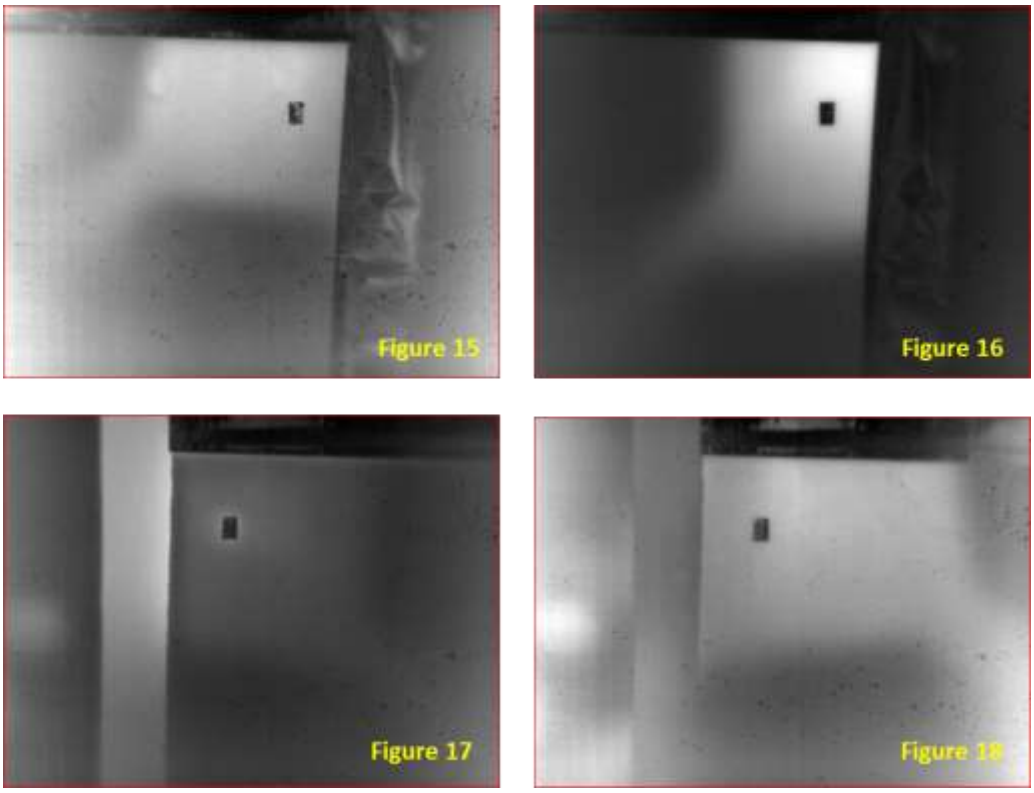

Figures 15, 16, 17 and 18: the image of the C-zone of the specimen taken by external transmisión (figure 15) and the image of the C-zone of the specimen taken by external reflection (figure16) The figure 17 and 18 corresponding to an image of the C-zone of the specimen taken by internal transmisión and image of the C-zone of the specimen taken by internal reflection respectively.

Radome analysis

The thermographs shown below have been obtained on the original piece to be inspected. Images of tests carried out on the same piece are shown, where the goodness of the method will be fine-tuned for the detection, mainly, of cracks and delaminations in the material, as well as identification of areas of resin accumulation and air pockets, those that have been called 'possible defects'.

In the thermographies carried out, some dark rectangular marks can be observed that correspond to references of 50mm x 5 mm made in aluminium tape, for the visual determination of the size of the possible defects.

Next, several areas in the part with different defects will be differentiated, and what happens when the part is inspected by active thermography will be analysed using the different forms of heating and image display, mentioned above, to analyse the thermal transient in the part.

4 Discussion

Identification of cracks

Figure 19 corresponds to a thermography obtained by external transmission, now the painted part of the radome is seen by the camera, and the unpainted part is heated. In this figure a longitudinal indication of dark colour can be seen that goes from the upper part of the image to the lower part. This indication probably corresponds to a crack repaired by accumulation of resin on it. Transversally to it, and as very fine white lines, other cracks in the piece are identified, probably not identified in a first visual inspection and not repaired. In the lower part of the image, a white line appears with a higher contrast than the previous indications, but in this case, it corresponds to the separation joint between the different panels of Rohacell material (not a defect). Dark spots also appear, but with lower contrast than the longitudinal mark, corresponding to dry areas of the piece, i.e. areas with less resin.

In figure 20, you can also see the dark longitudinal stain, but with less contrast than in figure 19. In this case, the cracks are not so clearly observed, and in some cases, they are not visible. The separation joint is also not visible. The heating and observation on this side seems to be at a disadvantage compared to the process used in thermography in figure 19.

In figure 21, it has been heated on the paint side and observed on the unpainted side. It can be commented that the references (dark rectangular stains) can be seen, even though they are placed on the other side of the piece. The longitudinal indication appears with less contrast to figure 19, but the indications of the cracks (fine white lines) are well defined.

Figures 19, 20, 21 and 22: Picture of indications on the part by external transmisión (figure 19) and the figure 20 is a illustration of the part by external reflection. For other hand, the figure 21 is a picture of indications on the part by internal transmisiónan the figure 22is an image of indications on the part by internal reflection.

The thermography in figure 22 shows the internal structure of the camera (radome), and the above indications are not visible, since they are on the other side of the inspected part, that is, the opposite side of the one observed by the infrared sensor.

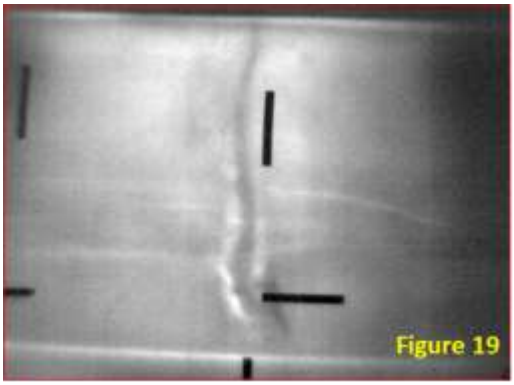

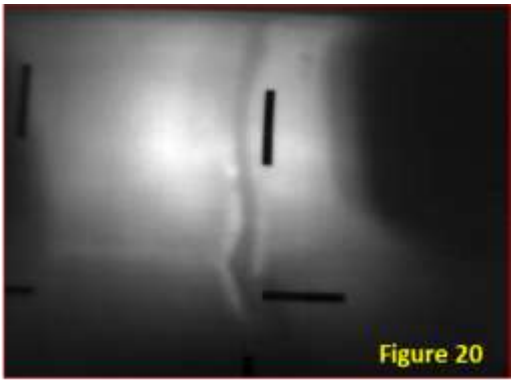

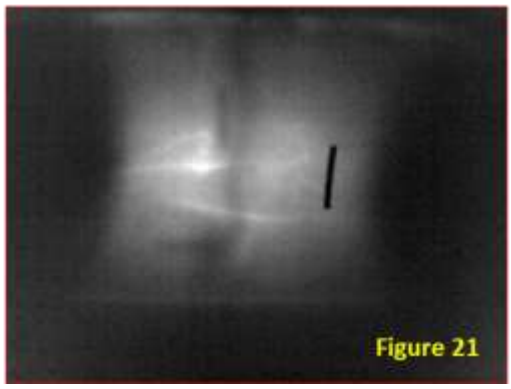

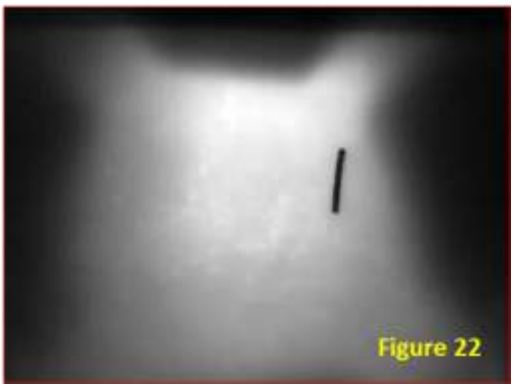

In figure 23, there are two vertical indications in dark colour, and another dark area in the lower part of the analysed area. With regard to the vertical indications, it can be noted that the repaired crack on the part can be seen with the naked eye, which is the crack on the right, but the other vertical indication next to it cannot be seen. By means of this technique, it does become evident. The dark spot at the bottom corresponds to an area of the part where little resin has been applied (dry area). There you can see folds in the fabric.

In the thermography of figure 24 only the lower indication appears and with less contrast, which may indicate that the indication, or zone of little resin, may be more towards the outside than the vertical indications.

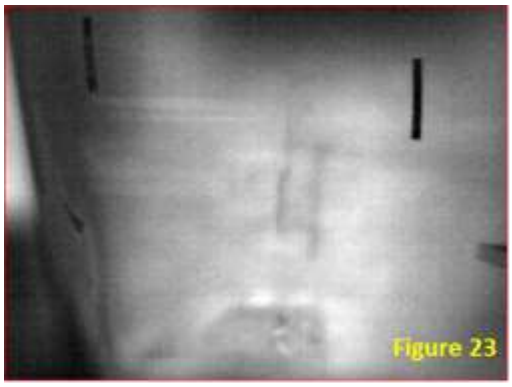

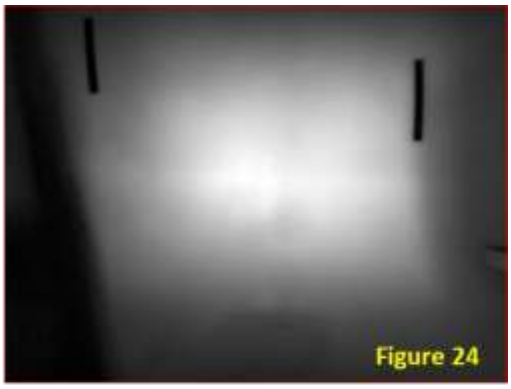

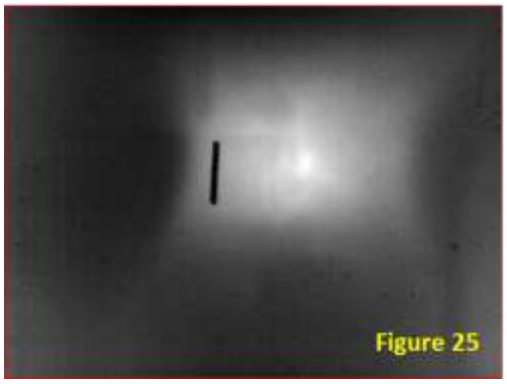

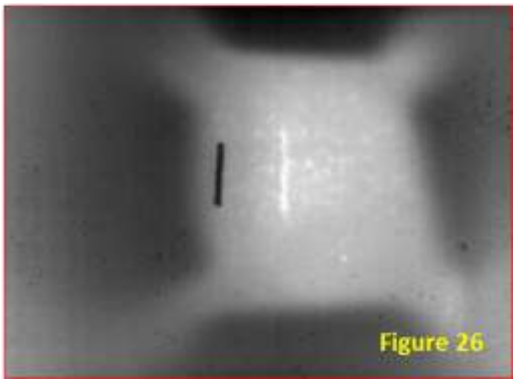

Figures 23, 24, 25 and 26: image of cracks in the piece due to external transmisión (figure 23), image of cracks in the part by external reflection (figure 24), image of cracks in the part by internal transmisión (figure 25) and mage of cracks in the piece by internal reflection (figure 26).

In figure 25 the vertical indications are not clearly visible, so it can be concluded that they are closer to the painted surface.

In figure 26, the crack located more to the right appears and it does it in white color. Now it is observed by the most favorable side to be seen, since at simple sight it is observed by this side. There are also some white lumps belonging to the internal structure of the piece.

Figure 27 shows, in the upper left part, a series of white lines with different inclinations, corresponding to the crack itself and its branches. Below, as a longitudinal line of greater contrast in white, the joint of the piece appears. In figure 28, the crack is shown in a very diffuse way and with little contrast as it is a core break. Figure 29 shows the crack in a very detailed way with all the branches. In figure 30, there are no indications, except for an area of lumps which give more indication, greater contrast, than the crack itself.

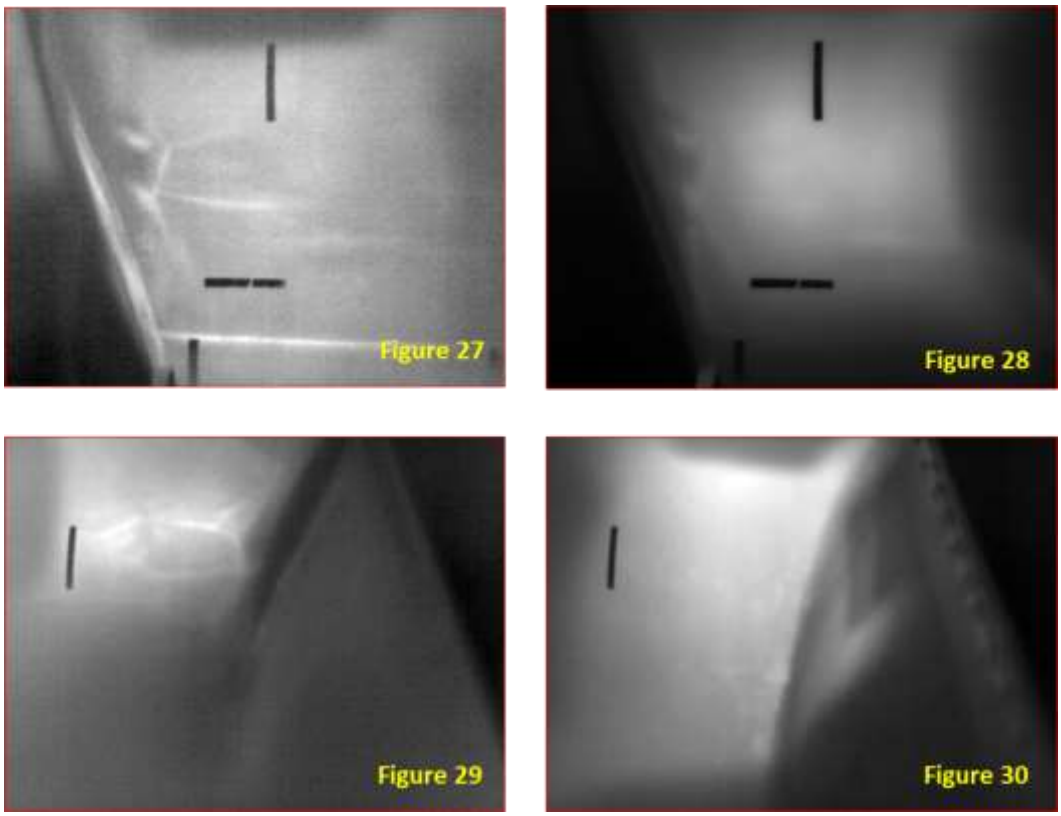

Figure 27,28,29 and 30: Branch image of a crack in the part by external transmisión (figure 27). Branch image of a crack in the part by external reflection (figure28). Image of branching of a crack in the part by internal transmisión (figure 29) and branch image of a crack in the part by internal reflection (figure 30).

Identification of delaminations

In order to study the delaminations in the monolithic material part of the piece (side areas of lesser thickness), small air pockets have been made between two very thin Teflon-type materials and placed behind and in front of the surface to be inspected, so that the goodness of the method for detecting this type of defect in this particular material (fibreglass) could be determined.

The manufacture of this type of defect has been carried out by hand. For this purpose, air pockets have been created by means of a release agent, surrounded by tape all around, in such a way that no air enters the delaminated area. Two 'delaminated zones' have been placed, one in the part of the piece to be inspected closer to the chamber, and the other, above it, in the part furthest away, that is, closer to the focus. The arrangement of both delaminated zones is shown in Figure 31.

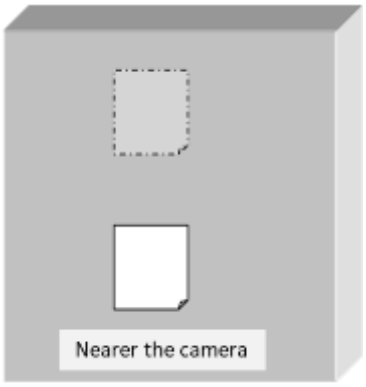

Figure 31: Diagram of delaminations in the piece.

The results obtained will be shown in the following thermographies.

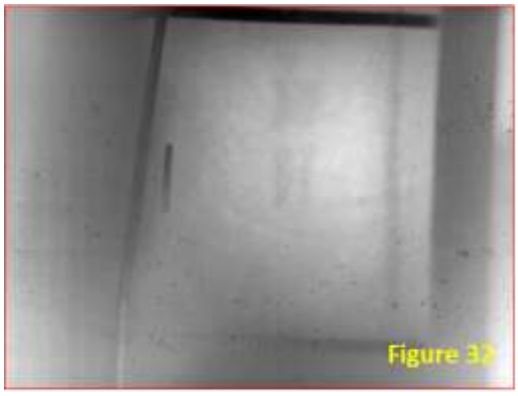

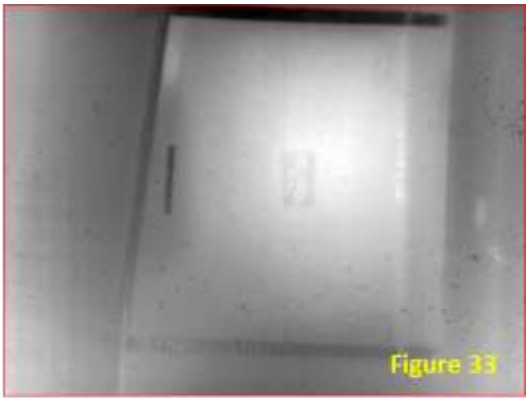

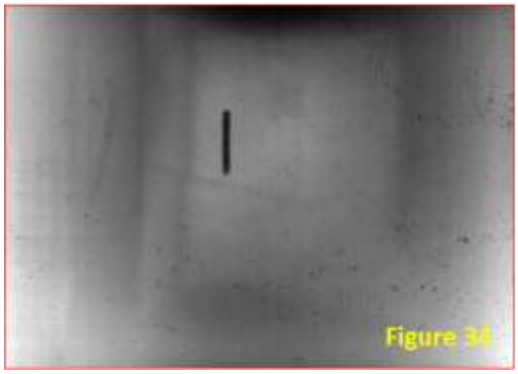

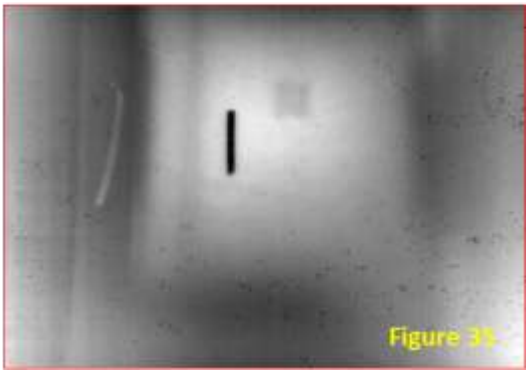

Figure 32,33,34 and 35. Image of delaminations in the monolithic part by external transmisión (figure 32). Image of delaminations in the monolithic of the part by external reflection (figure 33). Image of delaminations in the monolithic of the piece by internal transmisión (figure 34) and image of delaminations in the monolithic of the piece by internal reflection (figure 35).

Figure 32 shows the monolithic part of the piece where two rectangular zones appear in a slightly darker colour than the background. The lower rectangular area is slightly more diffused than the upper one, although it is the area that is being seen directly with the camera. This may be due to the fact that this area of delamination created has more air pockets than the one at the back.

Figure 33 shows the lower delaminated area. From the upper zone (delaminations on the back) there are no indications. Figure 34 shows nothing. Neither of the two delaminated areas can be seen. Figure 35 shows the upper delaminated area. In this case, it is now the most favorable area to be seen.

Identification of air pockets and material accumulation zones

The determination of air pockets and material accumulation, in this case resin, are shown in the following thermographies. The light coloured zones correspond to air pockets, as they are zones of higher temperature; in these zones the heat propagation is slower than if it was a zone of homogeneous material. The resin accumulation zones appear as dark spots, colder than the previous ones.

The thermography on the left, in figure 36, corresponds to the moment before the piece is heated. The study zone, in this case the edge of the piece is at room temperature. The thermography on the right corresponds to the heated edge after the heat pulses. It shows irregular spots corresponding to the air and resin pockets.

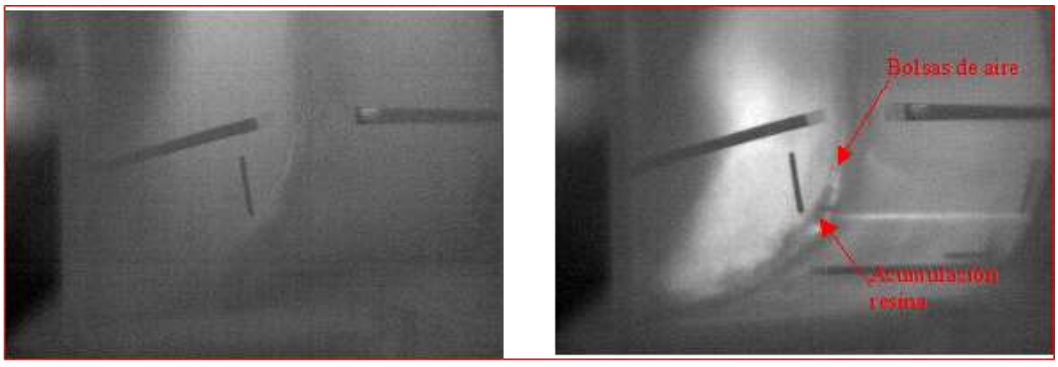

Figure 36: Air and resin pockets on the edge of the part (right-hand thermograph).

The thermography on the right, in figure 37, shows two dark spots in the central zone due to 'dry zones' with very little resin application, it is another type of detected irregularities in the surface of the part.

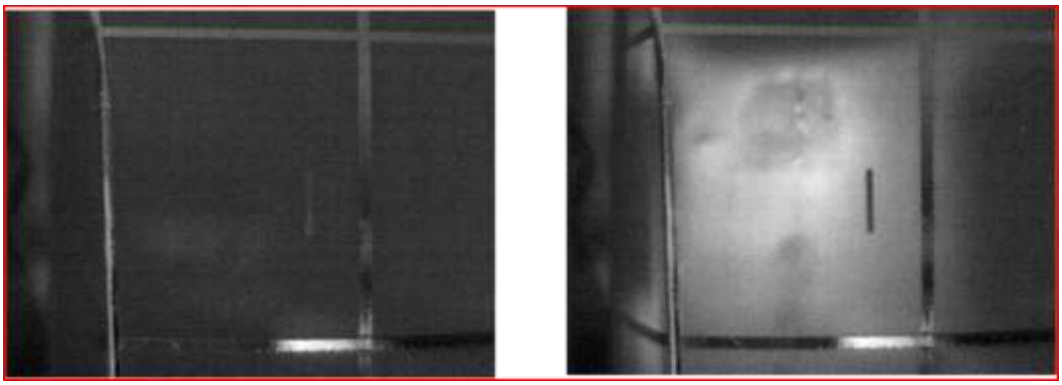

Figure 37: Material accumulation stains and folds in the part.

5 Conclusion

One of the most attractive advantages of thermal NDT methods, in this case pulse-thermography, is the possibility of scanning the sample (radome) without the need for physical contact with it, in the case of parts with complex geometric shape, difficult to access or hot, or to be able to perform the scan quickly thanks to non-contact heat sources and thermal sensors and IR cameras.

It has been shown that the pulse-thermography methodology is valid for inspecting fibreglass materials of small thicknesses and to be able to determine, with a correct setting of the method, important defects such as cracks and delaminations in this type of material.

It has also been demonstrated that it is possible to determine areas of material accumulation and air pockets that could rethink whether the manufacturing method is appropriate and thus the realization of a new design.
After analyzing the results obtained, it can be concluded that the most appropriate methodology to use for the detection of indications (defects) in this type of piece and specific material, has been the external transmission pulse-thermography. It is by this method that most of these defects are revealed, as they appear with greater contrast to the other methods (internal transmission, external reflection and internal reflection).

Once the method has been perfected, it can be concluded that it is a fast method for inspecting large parts, they are inspections without contact with the part, and have a wide range of applications in almost all sectors of industry.

Inspection by other non-destructive methods, such as ultrasound, X-ray, eddy currents, etc., could enrich the information obtained by this technology.

Acknowledgements. To the Materials Department of the National Institute of Aero Technology

References

[1] Product Showcase, *Infrared Testing*, Material Evaluation, 1987, p. 45.

[2] C. Hobbs, D. Kenway-Jackson, J. Milne, *Quantitative measurement of thermal parameters over large areas using Pulse Video Thermography*, Oxford 1991, Proceeding of SPIE Vol. 1467 Thermosense XIII, 264-277.

[3] D. González, F. Madruga, M. Quintela, J. López-Higuera, Defect assessment on radiant heaters using infrared thermography, *NDT&E International*, **38** (6) (2005), 428-432. https://doi.org/10.1016/j.ndteint.2004.11.006

[4] D.P. Almond, P. Delpech, M.H. Beheshtey. Wen P., Quantitative Determination ot Impact damage and Other Defects in Carbon Fiber Composites by Transient Thermography, *Procceeding of SPIE*, Vol. 2944, Bellingham, 1996, 256-264.

[5] E. Barreira, V. Freitas, Evaluation of building materials using infrared thermography, *Construction and Building Materials*, **21** (1) (2007), 218-224. https://doi.org/10.1016/j.conbuildmat.2005.06.049

[6] G. Delojo, J.M. Álvarez, J.A. Peñaranda, G. Sanglier, Estudio mediante ensayos no destructivos de la cubierta (‘radomo’) de un Sistema experimental de radar de apertura sintética, *Asociación Española de Ensayos No Destructivos. 10º Congreso Nacional de E.N.D.*, 2013, 39-45.

[7] G. Wu, F. Song, D. Li, Infrared temperature measurement and simulation of temperature field on buried pipeline leakage, *ICPTT* 2009, 203-209.

[8] M. Rahimi, A. Sabernaeemi, Experimental study of radiation and free convection in an enclosure with a radiant ceiling heating system, *Energy and Buildings*, **42** (11) (2010), 2077-2082 https://doi.org/doi:10.1016/j.enbuild.2010.06.017

[9] P. Annan, *GPR Principles procedures and applications*, Sensors and Software Inc., 2003.

[10] P. Brady Robert, R. Kulkarni Manohar, A Novel Pulsed Video Thermography Apparatus for the Quantitative Characterization of Material Flaws, Southern Illinois University, *Transactions of the Illinois State Academy of Science*, **88** (1995), 131-136.

[11] P. Cielo, X. Maldague, A.A. Déom, R. Lewark, Thermographic Non Destructive Evaluation of Industrial Material and Estructures, *Materials Evaluatión*, 1987, p. 45.

[12] P. Vvilov, P. Vladimir, Tree-dimensional analysis of transient thermal NDT problems by data simulation and processing, Orlando, Florida. Thermosense XXII, *Proceeding of SPIE*, Abril 2000, 152-173.

[13] S. Lagüela, H. González-Jorge, J. Armesto, J. Herráez, High performance grid for the metric calibration of thermographic cameras, *Measurement Science and Technology*, **23** (1) (2012), 015402
https://doi.org/10.1088/0957-0233/23/1/015402

[14] S. Lagüela, J. Armesto, P. Arias, J. Herráez, Automation of thermographic 3D modeling through image fusion and image matching techniques, *Automation in Construction*, **27** (2012), 24-31. https://doi.org/10.1016/j.autcon.2012.05.011

[15] T. Clausting, What you really need to know to begin using infrared cameras, *Materials Evaluation*, **64** (5) (2006), 465-470.

[16] T. Jones, H. Berger, *Thermographic detection of impact damage in graphite-epoxy composites*, Industrial Quality, Inc. 19634. Materials Evaluation, 1992, 321-356.

[17] V. Vavilov, Thermal NDT: Historical milestones, state-of-the-art and trends, *Quantitative InfraRed Thermography Journal*, **11** (1) (2014), 66-83. https://doi.org/10.1080/17686733.2014.897016

Received: March 21, 2020; Published: April 4, 2020